eawe
european academy of wind energy
10th PhD Seminar on Wind Energy in Europe
28-31 October 2014, Orléans, France

Is blade element momentum theory (BEM) enough for smart rotor design

Wei Yu[1], Carlos Simão Ferreira[1], G.A.M van Kuik[1]
[1]Delft University of Technology, Wind Energy,
Kluyverweg 1, 2629 HS, Delft, The Netherlands
E-mail: W.Yu@tudelft.nl

INTRODUCTION

Smart rotor emerges as an innovation technique to reduce the impact of dynamic loading on wind turbines. Local movements of distributed aerodynamic devices will enhance the non-uniformity and dynamic effects of loading, which will challenge the applicability of the blade element momentum theory (BEM) for smart rotor control design due to its fundamental assumptions, quasi-steady state and independent annuli. From a recent report of Sandia Lab of field tests of wind turbine with trailing edge flaps, an unsteady aerodynamic model for the response to turbulent wind and AALC device actuation is needed and a dynamic wake model is necesary[1]. However, most of previous aeroseverelastic studies of smart rotor are based on BEM or BEM-based engineering dynamic inflow models, none of them verify the applicability of BEM for smart rotor study.

In this paper, a free wake model which combined a vortex ring model with a semi-infinite cylindrical vortex tube is developed, and applied to an actuator disc with non-uniform and dynamic loading. After tested in a steady, uniform load case, the model is applied to three main load cases: a non-uniform steady load, a uniform dynamic load and a non-uniform dynamic load. Results from this model are compared with MT, and with two widely used engineering dynamic inflow models.

METHODOLOGY

For incompressible, inviscid fluid, the motion of the fluid particles is controlled by the Euler equation

$$\rho \frac{Du}{Dt} = -\nabla p + f \tag{1}$$

and the continuity equation:

$$\nabla \cdot u = 0 \tag{2}$$

In axial and axi-symmetric flow, the force on the actuator disc can be represented by a constant pressure jump Δp at the disc. van Kuik[2] obtained a relationship between vortex strength and pressure jump at the edge :

$$\frac{D\Gamma_{edge}}{Dt} = \frac{\Delta p}{\rho} \tag{3}$$

To model the vortex surface as discrete vortices we use vortex rings shed from any radial location of the disc's surface where the local pressure gradient is non-zero. The vortex rings are considered as thin, axi-symmetric and uniform. Axi-symmetric rings means that rings may expand or contract, but their centre lines will always coincide with the axis of actuator disc. The wake system is split into two parts: the near wake and the far wake part. The far wake is represented by a semi-infinite cylindrical vortex tube with constant strength and radius, whilst the near wake is modelled by dynamic surfaces, consisted of free vortex rings shed from the edge of the actuator disc or where a local load changes.
The analytical formulas for the velocity field induced by an infinitely thin axi-symmetric vortex ring are given by Yoon and Heister[3]. Figure 1 shows the cartesian coordinate system used in this paper. When the actuator disc is located at the z = 0 plane with the centreline along z axis, the axial and radial velocities at an arbitrary point P in the field induced by the ith vortex ring are given as:

$$V_z = \frac{\Gamma_i}{2\pi\sqrt{(z_p - z_i)^2 + (r_p + R_i)^2}}\left[K(m) + \frac{R_i^2 - r_p^2 - (z_p - z_i)^2}{(z_p - z_i)^2 + (r_p - R_i)^2}E(m)\right] \quad (4)$$

$$V_r = -\frac{(z_p - z_i)\Gamma_i}{2\pi r_p\sqrt{(z_p - z_i)^2 + (r_p + R_i)^2}}\left[K(m) - \frac{R_i^2 + r_p^2 + (z_p - z_i)^2}{(z_p - z_i)^2 + (r_p - R_i)^2}E(m)\right] \quad (5)$$

Where $< z_p, r_p >$ are coordinates of point P in the field where the velocity is to be calculated, $< z_i, R_i >$ is the axial coordinate and radius of the i^{th} vortex ring. K(m) and E(m) are the complete elliptic integrals of the first, second kind, where m is defined by $m = 4r_pR_i / [(z_p - z_i)^2 + (r_p + R_i)^2]$.
Several empirical dynamic inflow models were developed to correct BEM by previous researchers. Two of the most commonly used models among these : the Pitt-Peters dynamic inflow model[4] and the Øye dynamic inflow model (see the work of Snel and Schepers[5]), are chosen to compare with in the dynamic loading cases.

RESULTS

Here are some preliminary results from this study. Figure 2 compares the change of the averaged axial induction factor (*a*) at the actuator disc as a function of time calculated from the FWVR model and from the MT for different uniform, steady thrust efficiencies. The time scale used is non-dimensionalized using $\tau = V_0 t / R$. We can see the average *a* at the actuator plane from the FWVR model converges to ideal values of MT after different time periods for different thrusts. This proves the feasibility of the newly developed FWVR for aerodynamic load calculation.

For the steady non-uniform load, there are three steady load cases: uniform load C_t =7/9 at the actuator disc, a step increase and a step decrease of 1/9 in C_t at annulus of 0.6R - 0.8R. Figure 3 compares the distribution of the *a* at the actuator disc plane obtained from the FWVR model and MT for all the three load cases, after nondimensional time τ = 40. The axial induction factor calculated from the FWVR model matches very well with that from MT in general, though it's not as uniform as MT predicts, especially at the edge of actuator disc. For the step decreased load case, the locally changed *a* captured by the FWVR model matches that from MT, but for the step increased load case, the locally increased *a* obtained from the FWVR model does not reach the ideal value from MT.

For the unsteady uniform load, the thrust on the actuator disc is undergoing harmonic oscillations with an amplitude of ΔC_t=1/9 for different frequencies *w*. When the radius is treated as the characteristic length for the actuator disc, the reduced frequency is obtained from $k = wR / 2V_0$. Oscillations start at τ = 40 when the wake system of the uniform steady thrust (C_t = 7/9) approaches an equilibrium state. Simulations are presented for k = 0.05 in figure 4, it compares the hysteresis loops of the averaged *a* at the actuator disc of the FWVR model, MT, MT with the Pitt-Peters and the Øye dynamic inflow model. The dynamic *a* is plotted against thrust coefficient at the actuator disc. A discrepancy of the averaged *a* of the FWVR model from MT is seen at the beginning of the transient part, because an infinite long time is needed for the wake of the FWVR model to develop fully to approach the wake of MT model (which is also reflected in figure 2). In simulations, oscillations start at τ = 40 when the difference of *a* of the FWVR model from MT is 2.4% for C_t = 7/9. Since MT is based on the static state, it can not predict any dynamic effect, it's plotted here for comparison. As seen for k = 0.05, the amplitude of *a* predicted by the Pitt-Peters model matches with the quasi-steady values from the MT, but has a small phase lag (width of the hysteresis loop) from MT. The Øye model predicts a larger phase lag and amplitude difference (difference of width of *a* from that of the MT) than the Pitt-Peters dynamic inflow model, and the FWVR model predicts a even larger phase lag and amplitude difference than the Øye model.

For the non-uniform dynamic load, only the thrust at annulus of 0.6R -0.8R is undergoing harmonic oscillations with an amplitude of ΔC_t = 1/9 for a reduced frequency of 0.05. Oscillations also start at time τ = 40. Figure 5 compares hysteresis loops of the unsteady *a* at 0.7R (the center of load locally changed region) among the FWVR model, MT, MT with the Øye and the Pitt-Peters model. The dynamic induction *a* is plotted against the thrust coefficient at 0.7R. Loops of *a* at the local annulus predicted by the Øye and the Pitt-Peters model have a similar pattern as for the uniform dynamic load case. However, there is almost no hysteresis in the local induction *a* from the FWVR model.

CONCLUSION

A new free wake model is developed for the calculation of the induced velocity field of an actuator disc with non-uniform and dynamic loading. The model is composed of a free wake vortex ring model for the near wake and a semi-infinite cylindrical vortex tube for the far wake. Firstly, the model is verified in a steady and uniformly loaded state. The FWVR model is applied to three kinds of load cases: a non-uniform steady load, a uniform dynamic load and a non-uniform dynamic load case; comparisons of the results predicted by the FWVR model with MT, and the Pitt-Peters and the Øye dynamic inflow models in the dynamic load cases, shows that:

- The Momentum Theory and the independent annuli assumption is acceptable for steady non-uniform loads, though there is a small impact of local change in load outside the region where this load change occurs.
- Unsteady models are necessary for dynamic loading from uniform dynamic load cases.
- Both engineering dynamic inflow models based on the assumption of independent annuli are not applicable for investigations of the non-uniform dynamic loading.

REFERENCES

[1] J.C. Berg, M.F. Barone, N.C. Yoder. Smart wind turbine rotor: data analysis and conclusions. Sandia Report, SAND 2014-0712, Jan., 2014.

[2] G.A.M. van Kuik. The edge singularity of an actuator disc with a constant normal load. In 22nd AIAA/ASME Wind Energy Symposium, Reno USA, 2003.

[3] S.S. Yoon and S.D. Heister. Analytical formulas for the velocity field induced by an infinitely thin vortex ring. Int. J.Numer. Meth.Fluids, 44:665–672, 2004.

[4] D.M. Pitt and D.A. Peters. Theoretical prediction of dynamic-inflow derivatives*. Vertica, 5(1) :21–34, 1981.

[5] H. Snel and J.G. Schepers. Joint investigation of dynamic inflow effects and implemention of an engineering method. Technical report, 1995.

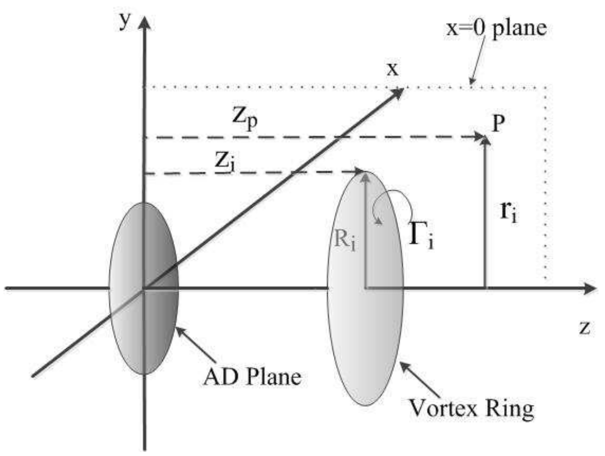

Figure 1. A schematic of coordinate system for computing induced velocity at arbitrary field points

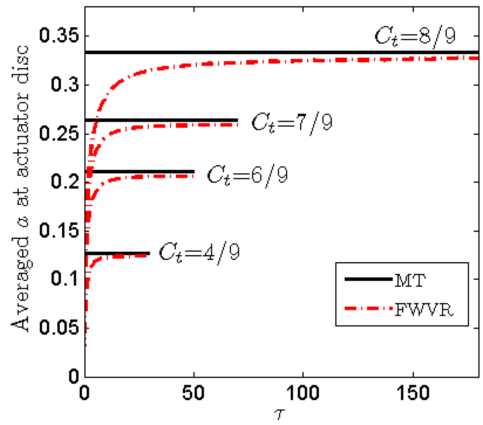

Figure 2. Comparison of averaged axial induction factor *a* at the actuator disc between the FWVR model and MT for different C_t

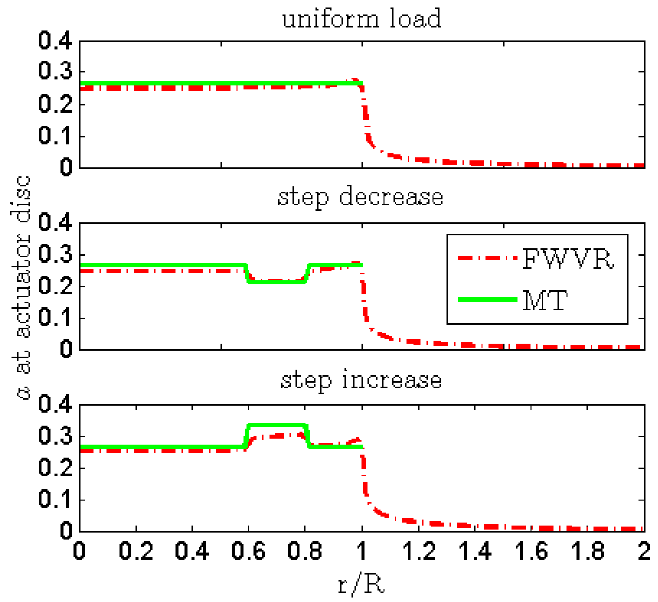

Figure3. Comparison of the distribution of *a* at actuator disc plane between the FWVR model and MT for non-uniform steady load

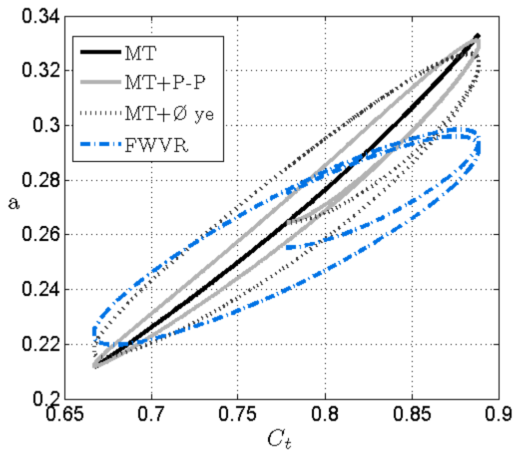

Figure 4. Comparison of hysteresis loops of averaged *a* at the actuator disc among the FWVR model, MT, MT with the Øye and the Pitt-Peters dynamic inflow model for an actuator disc undergoing harmonic thrust oscillations with an amplitude of ΔC_t = 1/9 for k = 0.05.

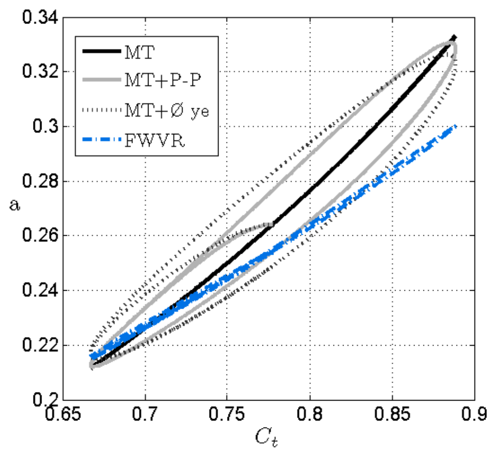

Figure 5. Comparison of hysteresis loops of *a* at 0.7R among the FWVR model, MT, MT with the Øye and the Pitt-Peters dynamic inflow model for an actuator disc undergoing harmonic thrust oscillations in the annulus region 0.6R - 0.8R with an amplitude of ΔC_t = 1/9 for k = 0.05.